

Search for Nucleon and Di-nucleon Decays with an Invisible Particle and a Charged Lepton in the Final State at the Super-Kamiokande Experiment

V. Takhistov,⁷ K. Abe,^{1,30} Y. Haga,¹ Y. Hayato,^{1,30} M. Ikeda,¹ K. Iyogi,¹ J. Kameda,^{1,30} Y. Kishimoto,^{1,30} M. Miura,^{1,30} S. Moriyama,^{1,30} M. Nakahata,^{1,30} T. Nakajima,¹ Y. Nakano,¹ S. Nakayama,^{1,30} A. Orii,¹ H. Sekiya,^{1,30} M. Shiozawa,^{1,30} A. Takeda,^{1,30} H. Tanaka,¹ T. Tomura,^{1,30} R. A. Wendell,^{1,30} T. Irvine,² T. Kajita,^{2,30} I. Kametani,² K. Kaneyuki,^{2,30,*} Y. Nishimura,² E. Richard,² K. Okumura,^{2,30} L. Labarga,³ P. Fernandez,³ J. Gustafson,⁴ C. Kachulis,⁴ E. Kearns,^{4,30} J. L. Raaf,⁴ J. L. Stone,^{4,30} L. R. Sulak,⁴ S. Berkman,⁵ C. M. Nantais,⁵ H. A. Tanaka,⁵ S. Tobayama,⁵ M. Goldhaber,^{6,*} G. Carminati,⁷ W. R. Kropp,⁷ S. Mine,⁷ P. Weatherly,⁷ A. Renshaw,⁷ M. B. Smy,^{7,30} H. W. Sobel,^{7,30} K. S. Ganezer,⁸ B. L. Hartfiel,⁸ J. Hill,⁸ N. Hong,⁹ J. Y. Kim,⁹ I. T. Lim,⁹ A. Himmel,¹⁰ Z. Li,¹⁰ K. Scholberg,^{10,30} C. W. Walter,^{10,30} T. Wongjirad,¹⁰ T. Ishizuka,¹¹ S. Tasaka,¹² J. S. Jang,¹³ J. G. Learned,¹⁴ S. Matsuno,¹⁴ S. N. Smith,¹⁴ M. Friend,¹⁵ T. Hasegawa,¹⁵ T. Ishida,¹⁵ T. Ishii,¹⁵ T. Kobayashi,¹⁵ T. Nakadaira,¹⁵ K. Nakamura,^{15,30} Y. Oyama,¹⁵ K. Sakashita,¹⁵ T. Sekiguchi,¹⁵ T. Tsukamoto,¹⁵ A. T. Suzuki,¹⁶ Y. Takeuchi,^{16,30} T. Yano,¹⁶ S. Hirota,¹⁷ K. Huang,¹⁷ K. Ieki,¹⁷ T. Kikawa,¹⁷ A. Minamino,¹⁷ T. Nakaya,^{17,30} K. Suzuki,¹⁷ S. Takahashi,¹⁷ Y. Fukuda,¹⁸ K. Choi,¹⁹ Y. Itow,¹⁹ T. Suzuki,¹⁹ P. Mijakowski,²⁰ K. Frankiewicz,²⁰ J. Hignight,²¹ J. Imber,²¹ C. K. Jung,²¹ X. Li,²¹ J. L. Palomino,²¹ M. J. Wilking,²¹ C. Yanagisawa,^{21,†} H. Ishino,²² T. Kayano,²² A. Kibayashi,²² Y. Koshio,²² T. Mori,²² M. Sakuda,²² Y. Kuno,²³ R. Tacik,^{24,32} S. B. Kim,²⁵ H. Okazawa,²⁶ Y. Choi,²⁷ K. Nishijima,²⁸ M. Koshihara,²⁹ Y. Suda,²⁹ Y. Totsuka,^{29,*} M. Yokoyama,^{29,30} C. Bronner,³⁰ M. Hartz,³⁰ K. Martens,³⁰ Ll. Marti,³⁰ Y. Suzuki,³⁰ M. R. Vagins,^{30,7} J. F. Martin,³¹ P. de Perio,³¹ A. Konaka,³² S. Chen,³³ Y. Zhang,³³ and R. J. Wilkes³⁴

(The Super-Kamiokande Collaboration)

¹Kamioka Observatory, Institute for Cosmic Ray Research, University of Tokyo, Kamioka, Gifu 506-1205, Japan

²Research Center for Cosmic Neutrinos, Institute for Cosmic Ray Research, University of Tokyo, Kashiwa, Chiba 277-8582, Japan

³Department of Theoretical Physics, University Autonoma Madrid, 28049 Madrid, Spain

⁴Department of Physics, Boston University, Boston, MA 02215, USA

⁵Department of Physics and Astronomy, University of British Columbia, Vancouver, BC, V6T1Z4, Canada

⁶Physics Department, Brookhaven National Laboratory, Upton, NY 11973, USA

⁷Department of Physics and Astronomy, University of California, Irvine, Irvine, CA 92697-4575, USA

⁸Department of Physics, California State University, Dominguez Hills, Carson, CA 90747, USA

⁹Department of Physics, Chonnam National University, Kwangju 500-757, Korea

¹⁰Department of Physics, Duke University, Durham NC 27708, USA

¹¹Junior College, Fukuoka Institute of Technology, Fukuoka, Fukuoka 811-0295, Japan

¹²Department of Physics, Gifu University, Gifu, Gifu 501-1193, Japan

¹³GIST College, Gwangju Institute of Science and Technology, Gwangju 500-712, Korea

¹⁴Department of Physics and Astronomy, University of Hawaii, Honolulu, HI 96822, USA

¹⁵High Energy Accelerator Research Organization (KEK), Tsukuba, Ibaraki 305-0801, Japan

¹⁶Department of Physics, Kobe University, Kobe, Hyogo 657-8501, Japan

¹⁷Department of Physics, Kyoto University, Kyoto, Kyoto 606-8502, Japan

¹⁸Department of Physics, Miyagi University of Education, Sendai, Miyagi 980-0845, Japan

¹⁹Solar Terrestrial Environment Laboratory, Nagoya University, Nagoya, Aichi 464-8602, Japan

²⁰National Centre For Nuclear Research, 00-681 Warsaw, Poland

²¹Department of Physics and Astronomy, State University of New York at Stony Brook, NY 11794-3800, USA

²²Department of Physics, Okayama University, Okayama, Okayama 700-8530, Japan

²³Department of Physics, Osaka University, Toyonaka, Osaka 560-0043, Japan

²⁴Department of Physics, University of Regina, 3737 Wascana Parkway, Regina, SK, S4S0A2, Canada

²⁵Department of Physics, Seoul National University, Seoul 151-742, Korea

²⁶Department of Informatics in Social Welfare, Shizuoka University of Welfare, Yaizu, Shizuoka, 425-8611, Japan

²⁷Department of Physics, Sungkyunkwan University, Suwon 440-746, Korea

²⁸Department of Physics, Tokai University, Hiratsuka, Kanagawa 259-1292, Japan

²⁹The University of Tokyo, Bunkyo, Tokyo 113-0033, Japan

³⁰Kavli Institute for the Physics and Mathematics of the Universe (WPI), Todai Institutes for Advanced Study, University of Tokyo, Kashiwa, Chiba 277-8582, Japan

³¹Department of Physics, University of Toronto, 60 St., Toronto, Ontario, M5S1A7, Canada

³²TRIUMF, 4004 Wesbrook Mall, Vancouver, BC, V6T2A3, Canada

³³Department of Engineering Physics, Tsinghua University, Beijing, 100084, China

³⁴Department of Physics, University of Washington, Seattle, WA 98195-1560, USA

(Dated: October 8, 2018)

Search results for nucleon decays $p \rightarrow e^+ X$, $p \rightarrow \mu^+ X$, $n \rightarrow \nu \gamma$ (where X is an invisible, massless particle) as well as di-nucleon decays $np \rightarrow e^+ \nu$, $np \rightarrow \mu^+ \nu$ and $np \rightarrow \tau^+ \nu$ in the Super-Kamiokande experiment are presented. Using single-ring data from an exposure of 273.4 kton · years, a search for these decays yields a result consistent with no signal. Accordingly, lower limits on the partial lifetimes of $\tau_{p \rightarrow e^+ X} > 7.9 \times 10^{32}$ years, $\tau_{p \rightarrow \mu^+ X} > 4.1 \times 10^{32}$ years, $\tau_{n \rightarrow \nu \gamma} > 5.5 \times 10^{32}$ years, $\tau_{np \rightarrow e^+ \nu} > 2.6 \times 10^{32}$ years, $\tau_{np \rightarrow \mu^+ \nu} > 2.2 \times 10^{32}$ years and $\tau_{np \rightarrow \tau^+ \nu} > 2.9 \times 10^{31}$ years at a 90% confidence level are obtained. Some of these searches are novel.

PACS numbers: 12.10.Dm,13.30.-a,11.30.Fs,14.20.Dh,29.40.Ka

Many signs indicate that the Standard Model (SM) of particle physics is an incomplete description of nature. Gauge coupling unification, charge quantization and other features suggest a more unified account, such as a Grand Unified Theory (GUT) [1–4], as an underlying fundamental theory. While the unification scale ($\sim 10^{15} - 10^{16}$ GeV) is unreachable by accelerators, rare processes predicted by these theories, such as proton decay, can be probed by large underground detectors. Being a signature prediction of GUTs, observation of an unstable proton would constitute robust evidence for physics beyond the SM, while non-observation will stringently constrain theoretical models.

The simplest unification scenarios based on minimal SU(5) and supersymmetric (SUSY) SU(5) have been decisively ruled out by bounds on $p \rightarrow e^+ \pi^0$ [5–7] and $p \rightarrow \bar{\nu} K^+$ [8]. Many alternative scenarios as well as potential signatures are possible (see [9] for review).

In this *Letter*, we analyze a broad class of nucleon and di-nucleon decay channels with a showering or non-showering single Cherenkov ring signature within the Super-Kamiokande (SK) experiment, using the technique of spectral fit [10, 11]. First, we have considered two general two-body decays $p \rightarrow e^+ X$ and $p \rightarrow \mu^+ X$, where X is a single unknown invisible particle which is assumed to be massless. These searches are distinct from the model-dependent inclusive analyses of [12, 13] listed in the PDG [14]. Similarly, we also consider $n \rightarrow \nu \gamma$. Though this radiative process is suppressed, it has a clean signature and has been considered in the context of SU(5) [15], with some models [9] predicting a lifetime of $10^{38 \pm 1}$ years.

While single nucleon $\Delta B = 1$ processes have been in general well studied, di-nucleon $\Delta B = 2$ channels also pose great interest. These higher-dimensional processes can become significant in models which suppress proton decay and could be connected to baryogenesis [16], accounting for the observed baryon asymmetry of the universe [17]. Such a connection may already be hinted at from the requirement of baryon number violation as a necessary condition for explaining the asymmetry [18]. The disappearance $\Delta B = 2$ reactions, with invisible final state particles, have been studied and no signal excess was observed [19–21]. The channels $np \rightarrow e^+ \nu$, $np \rightarrow \mu^+ \nu$ and $np \rightarrow \tau^+ \nu$ violate baryon number by two units and violate lepton number by either two or zero units. They can become significant in models with

an extended Higgs sector [16, 22], which could be considered in the context of GUTs [23]. While the τ cannot occur in single nucleon decay, in di-nucleon decay the τ channel is allowed [24]. The process $np \rightarrow \tau^+ \nu$ has not been experimentally studied before and in addition to the electron and muon channel searches we present the first search in the τ channel.

In this work, SK data is analyzed from the data taking periods of SK-I (May 1996-Jul 2001, 1489.2 live days), SK-II (Jan 2003-Oct 2005, 798.6 live days), SK-III (Sept 2006-Aug 2008, 518.1 live days) and the ongoing SK-IV experiment (Sept 2008-Oct 2013, 1632.3 live days), corresponding to a combined exposure of 273.4 kton · years. The 50-kiloton SK water Cherenkov detector (22.5-kiloton fiducial mass) is located beneath a one-km rock overburden (2700m water equivalent) in the Kamioka mine in Japan. Details of the detector design and performance in each SK period, as well as calibration, data reduction and simulation information can be found in [25, 26]. This analysis considers only events in which all observed Cherenkov light was fully contained (FC) within the inner detector.

Since final-state neutrinos or X (by definition) are not observed, the only signature of $p \rightarrow e^+ X$, $p \rightarrow \mu^+ X$, $n \rightarrow \nu \gamma$, $np \rightarrow e^+ \nu$ and $np \rightarrow \mu^+ \nu$ is a single charged e^+ or μ^+ lepton, or single γ . Thus, the invariant mass of the initial state cannot be reconstructed and the signal will be superimposed on a substantial atmospheric neutrino background in the e -like and μ -like momentum spectra. For the $np \rightarrow \tau^+ \nu$ decay, only the $\tau \rightarrow e^+ \nu \nu$ and $\tau \rightarrow \mu^+ \nu \nu$ channels are considered, with the respective branching ratios of 17.8% and 17.4%. This allows us to perform all the analyses within a unified framework. The previous searches for $n \rightarrow \nu \gamma$, $np \rightarrow e^+ \nu$ and $np \rightarrow \mu^+ \nu$, which were performed with a smaller detector using a counting method, resulted in the lifetime limits of 2.8×10^{31} years [5], 2.8×10^{30} years [19] and 1.6×10^{30} years [19], respectively. In contrast, the spectral fit employed within this work, allows utilization of the extra information from the energy dependence of signal, background and the systematic errors. This methodology has been recently employed in the SK nucleon decay [11, 27] and dark matter analyses [28].

The nucleon decay signal events are obtained from Monte Carlo (MC) simulations, in which all the nucleons of the water H₂O molecule are assumed to decay with

equal probability. The final state particles are generated with energy and momentum uniformly distributed in phase space. The effects of Fermi motion, nuclear binding energy as well as nucleon - nucleon correlated decays [29] are taken into account for both nucleon [30–32] and di-nucleon searches [33]. The signal Fermi momentum distributions are simulated using a spectral function fit to electron- ^{12}C scattering data [34]. The SK detector simulation [26] is based on the GEANT-3 [35] package, with the TAUOLA [36] package employed for decaying the τ leptons. For the $np \rightarrow \tau^+\nu$ mode we generated three MC samples, with the τ decaying to $e^+\nu\nu$, $\mu^+\nu\nu$ and all decay channels. The latter allows us to study sample contamination in the two selected leptonic τ channels from the hadronic τ channels and thus identify sample purity after the event selection. We have confirmed that the resulting MC charged lepton spectra from $\tau \rightarrow e^+\nu\nu$ and $\tau \rightarrow \mu^+\nu\nu$ decays agree with the theoretical formula [37]. For $p \rightarrow e^+X$ and $p \rightarrow \mu^+X$ modes, the invisible X particle cannot be a fermion by spin conservation, but in our spin-insensitive MC it was simulated as a neutrino. In total, around 4,200 signal events were generated within the fiducial volume (FV) for each SK period for single nucleon decays and around 8,400 for di-nucleon decays.

Atmospheric neutrino background interactions were generated using the flux of Honda *et. al.* [38] and the NEUT simulation package [39], which uses a relativistic Fermi gas model. Background MC corresponding to a 500-year exposure of the detector was simulated for each detector phase. We used the same atmospheric neutrino MC as the standard SK oscillation analysis [40].

The event selection applied to the fully-contained data is the following: (A) a single Cherenkov ring is present, (B) the ring is showering (electron-like) for $p \rightarrow e^+X$, $n \rightarrow \nu\gamma$, $np \rightarrow e^+\nu$ and $np \rightarrow \tau^+\nu$ ($\tau \rightarrow e^+\nu\nu$) and non-showering (muon-like) for $p \rightarrow \mu^+X$, $np \rightarrow \mu^+\nu$ and $np \rightarrow \tau^+\nu$ ($\tau \rightarrow \mu^+\nu\nu$), (C) there are zero decay electrons for modes with an e -like ring and one decay electron for those with a μ -like ring, (D) the reconstructed momentum lies in the range $100 \text{ MeV}/c \leq p_e \leq 1000 \text{ MeV}/c$ for $p \rightarrow e^+X$, $n \rightarrow \nu\gamma$ and in the range $200 \text{ MeV}/c \leq p_\mu \leq 1000 \text{ MeV}/c$ for $p \rightarrow \mu^+X$, with the range extended to 100-1500 MeV/c for di-nucleon decays with an e -like ring and 200-1500 MeV/c for those with a μ -like ring. In total, approximately 37,000 FC events were obtained in the SK-I to SK-IV data-taking periods. After the criteria (A)-(D) have been applied, the final data samples for single nucleon decay searches with an e -like ring contain 8,500 events and 6,000 events for the case of μ -like ring, with momenta up to one GeV/c . To search for di-nucleon decays we consider lepton momenta up to 1500 MeV/c . The final samples for the di-nucleon modes contain 9,500 events for the e -like channels and 6,500 events for the μ -like ones. See Ref. [41] for details regarding reconstruction.

The signal detection efficiency is defined as the fraction of events passing selection criteria compared to the total number of events generated within the true fiducial volume. The average detection efficiency for e -like channels is $94.0 \pm 0.4\%$ for all SK data-taking periods. For the μ -like channels, the average detection efficiency is $76.4 \pm 0.6\%$ for SK-I to SK-III and $91.7 \pm 0.4\%$ for SK-IV. The increase in efficiency observed in SK-IV for channels with a μ -like ring, comes from a 20% improvement in the detection of muon decay electrons after an upgrade of the detector electronics [26].

For the studied e -like momentum spectrum up to 1500 MeV/c , the dominant background contribution, composing 75.8% of the events, comes from the ν_e charged-current (CC) quasi-elastic (QE) neutrino channel. The ν_e CC single-pion production constitutes 13.0% of the background, while the ν_e CC coherent-pion, CC multi-pion and neutral-current (NC) single-pion productions contribute around 1.1%, 1.1% and 1.6%, respectively. About 3.5% and 1.1% of events come from ν_μ NC single-pion and coherent-pion production. For the μ -like momentum spectrum up to 1500 MeV/c , the dominant contribution of around 78.6% comes from ν_μ CCQE. Similarly, ν_μ CC single-pion, CC coherent-pion and CC multi-pion as well as NC single-pion production contribute around 16.2%, 1.4%, 1.6% and 0.8%, respectively.

After event selection, a spectral fit is performed on the reconstructed charged lepton momentum distribution of the events. The χ^2 minimization fit is based on the Poisson distribution, with the systematic uncertainties accounted for by quadratic penalties (“pull terms”) [10]. The χ^2 function used in the analysis is

$$\chi^2 = 2 \sum_{i=1}^{\text{nbins}} \left(N_i^{\text{exp}} + N_i^{\text{obs}} \left[\ln \frac{N_i^{\text{obs}}}{N_i^{\text{exp}}} - 1 \right] \right) + \sum_{j=1}^{N_{\text{syserr}}} \left(\frac{\epsilon_j}{\sigma_j} \right)^2$$

$$N_i^{\text{exp}} = \left[\alpha \cdot N_i^{\text{back}} + \beta \cdot N_i^{\text{sig}} \right] \left(1 + \sum_{j=1}^{N_{\text{syserr}}} f_i^j \frac{\epsilon_j}{\sigma_j} \right), \quad (1)$$

where i labels the analysis bin. The terms N_i^{obs} , N_i^{sig} , N_i^{back} , N_i^{exp} are the numbers of observed data, signal MC, background MC and the total (signal and background) MC events in each bin i . The index j labels the systematic errors, while ϵ_j and f_i^j correspond to the fit error parameter and the fractional change in the N_i^{exp} bin due to 1-sigma error uncertainty σ_j , respectively. The fit is performed for two parameters α and β , which denote the background and signal normalizations, respectively. After the event selection, the signal MC distribution is normalized to the background by the integral, which in turn is normalized to the SK livetime. This allows us to identify the fit point $(\alpha, \beta) = (1, 0)$ with the no-signal hypothesis. Similarly, $(\alpha, \beta) = (0, 1)$ signifies that the data is described by signal only, with the signal amount

TABLE I: Best fit (α, β) parameter values, best fit χ^2 / d.o.f., no signal $\Delta\chi^2$, 90% C.L. value of β parameter, allowed number of nucleon decay events in the full 273.4 kton \cdot years exposure (SK-I: 91.7, SK-II: 49.2, SK-III: 31.9, SK-IV: 100.5) and a partial lifetime limit for each decay mode at 90% C.L.

Decay mode	Best fit	Best fit	No signal	Data	Data	Sensitivity	τ/\mathcal{B}
	(α, β)	$\chi^2/\text{d.o.f.}$	$\Delta\chi^2$	$\beta_{90\text{CL}}$	$N_{90\text{CL}}$	$(\times 10^{31} \text{ yr.})$	$(\times 10^{31} \text{ yr.})$
$p \rightarrow e^+ X$	(1.050, 0.002)	70.9/70	0.19	0.013	108	79	79
$n \rightarrow \nu\gamma$	(1.045, 0.004)	70.5/70	0.43	0.015	125	58	55
$p \rightarrow \mu^+ X$	(0.960, 0.016)	63.2/62	3.43	0.032	187	77	41
$np \rightarrow e^+ \nu$	(0.955, 0.000)	122.5/110	0.00	0.004	33	10	26
						(per nucleus)	(per nucleus)
$np \rightarrow \mu^+ \nu$	(0.910, 0.000)	97.0/102	0.00	0.005	36	11	20
						(per nucleus)	(per nucleus)
$np \rightarrow \tau^+ \nu$	(0.910, 0.000)	224.6/214	0.00	0.006	56	1	3
$(\tau \rightarrow e^+ \nu\nu)$							
$(\tau \rightarrow \mu^+ \nu\nu)$					40	(per nucleus)	(per nucleus)

TABLE II: Systematic errors of spectrum fits, with 1σ uncertainties and resulting fit pull terms. Errors specific to signal and background are denoted by S and B, while those that are common to both by SB.

Decay mode	$p \rightarrow e^+ X$		$p \rightarrow \mu^+ X$			
Systematic error	1- σ uncertainty (%)		Fit pull (σ)		Fit pull (σ)	
Final state interactions (FSI)	10		0.10		-0.60	B
Flux normalization ($E_\nu < 1$ GeV)	25 ^a		-0.23		-0.08	B
Flux normalization ($E_\nu > 1$ GeV)	15 ^b		-1.44		-0.50	B
M_A in ν interactions	10		0.69		0.23	B
Single meson cross-section in ν interactions	10		-0.55		-0.14	B
Energy calibration of SK-I, -II, -III, -IV	1.1, 1.7, 2.7, 2.3	0.58, -0.91, 0.48, 0.38	-0.54, 0.07, -0.14, 0.26			SB
Fermi model comparison	10 ^c		-0.08		0.70	S
Nucleon-nucleon correlated decay	100		0.00		0.06	S

^a Uncertainty linearly decreases with $\log E_\nu$ from 25% (0.1 GeV) to 7% (1 GeV).

^b Uncertainty is 7% up to 10 GeV, linearly increases with $\log E_\nu$ from 7% (10 GeV) to 12% (100 GeV) and then 20% (1 TeV).

^c Estimated from comparison of spectral function and Fermi gas model.

equal to background MC normalized (pre-fit) to livetime. The χ^2 minimization is carried out over each α and β in the grid according to $\partial\chi^2/\partial\epsilon_j = 0$. The resulting global minimum is defined as the best fit. Further details on the fit and specifics of systematic error treatment can be found in [11, 28, 42]. For the $np \rightarrow \tau^+ \nu\nu$ mode, after the appropriate event selection is applied to both MC samples of $\tau \rightarrow e^+ \nu\nu$ and $\tau \rightarrow \mu^+ \nu\nu$, the samples are combined for the fit, allowing us to obtain a single value for the permitted number of nucleon decays at 90% CL.

The systematic errors can be divided into signal-specific (S), background-specific (B) as well as detector and reconstruction errors, which are common to both signal and background (SB). The two signal specific systematics are from Fermi motion and nucleon - nucleon

correlated decay. For background, in order to methodically select the dominant systematics, we started from more than 150 errors employed in the SK oscillation analysis [42] and chose those which affect the analyses bins by more than 5% ($|f_i^j| \geq 0.05$). Relaxing this criteria to 1% does not significantly alter the results, but complicates the analysis [11]. As in [11], we have found that the dominant contributions originate from uncertainties related to neutrino flux and energy calibration (common to both signal and background). Including the signal systematics, the total number of considered errors is 11 and they are the same for all modes. In Table II we display the complete list of systematics, their uncertainties and fitted pull terms for two representative examples $p \rightarrow e^+ X$ and $p \rightarrow \mu^+ X$.

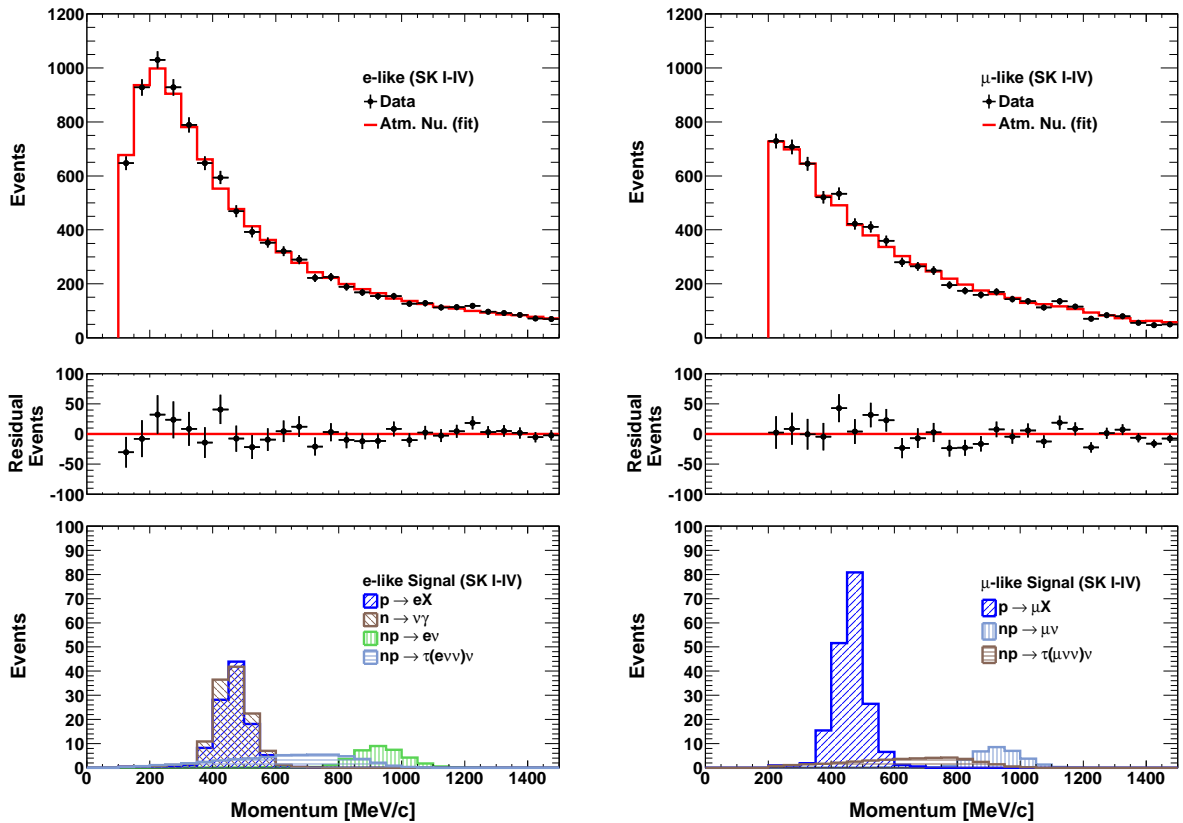


FIG. 1: [Top] Reconstructed momentum distribution for 273.4 kton · years of combined SK data (black dots) and the best-fit result for the atmospheric neutrino background Monte Carlo (solid line). The corresponding residuals are shown below, after fitted background subtraction from data. [Bottom] The 90% confidence level allowed nucleon decay signal (hatched histograms), from the signal and background MC fit to data. All modes are shown (overlaid), with e -like channels on the left and μ -like channels on the right.

The spectral fit determines the overall background and signal normalizations α and β , with the fit results displayed in Table I. The outcome shows that no significant signal excess has been observed, with the data $\Delta\chi^2 = \chi^2 - \chi_{min}^2$ being within 1σ of the background only hypothesis for all search modes except for $p \rightarrow \mu^+ X$, which is within 2σ .

The lower lifetime limit on the processes can then be computed from the 90% confidence level value of β (β_{90CL}), which translates into the allowed amount of signal at 90% confidence level according to $N_{90CL} = \beta_{90CL} \cdot N^{\text{signal}}$, where N^{signal} is the total number of signal events. The partial lifetime limit is then calculated from

$$\tau_{90CL}/\mathcal{B} = \frac{\sum_{\text{sk}=\text{SK1}}^{\text{SK4}} \lambda_{\text{sk}} \cdot \epsilon_{\text{sk}} \cdot N^{\text{nucleons}}}{N_{90CL}}, \quad (2)$$

where \mathcal{B} is the branching ratio of a process, ϵ_{sk} and λ_{sk} are the signal efficiency and the exposure in kton · years for each SK phase, N_{90CL} is the amount of signal allowed at the 90% confidence level and N^{nucleons} is the number of nucleons per kiloton of water, corresponding to 3.3×10^{32} ,

2.7×10^{32} and 3.3×10^{31} for proton, neutron and di-nucleon decay searches, respectively.

The resulting fitted spectra for the 273.4 kton · years of combined SK data can be found in Figure 1. The upper figures display best-fit result for atmospheric neutrino background (solid line) without signal fitted to data (black dots) and the corresponding residuals after the fitted MC is subtracted from data. It is seen that the background MC describes the data well. The bottom figures display the 90% C.L. allowed signal (hatched histogram), obtained from the fit of background with signal to data, with all the e -like and μ -like spectra overlaid with all the modes. The N_{90CL} as well as resulting sensitivities and calculated lifetime limits for the decays are shown in Table I. The sensitivities were obtained assuming that data are described by background. For the $np \rightarrow \tau\nu$ mode we have combined the τ channels $e^+\nu\nu$ and $\mu^+\nu\nu$, weighted by their respective branching ratios. This limit is then multiplied by 1.15 to account for roughly 85% sample purity of these channels. From the analyses we set the lower limits on the partial lifetimes of the decay modes at the 90% confidence level, with the results shown in Table I.

In conclusion, the single Cherenkov ring momentum spectra in Super-Kamiokande are well described by atmospheric neutrinos, including the effect of neutrino oscillation and systematic uncertainties, up to 1500 MeV/c. We find no evidence for any contribution from the six different nucleon and di-nucleon decay modes that would produce a showering or non-showering Cherenkov ring. The results of this analysis provide a stringent test of new physics. The obtained limits represent more than an order of magnitude improvement over the previous analyses of $n \rightarrow \nu\gamma$ [5] and two orders of magnitude for $np \rightarrow e^+\nu$ and $np \rightarrow \mu^+\nu$ [19]. The searches for $p \rightarrow e^+X$, $p \rightarrow \mu^+X$ (where X is an invisible, massless particle) and $np \rightarrow \tau^+\nu$ are novel. The di-nucleon decay limits restrict $\Delta B = 2$ processes with L violated by either zero or two units.

We gratefully acknowledge cooperation of the Kamioka Mining and Smelting Company. The Super-Kamiokande experiment was built and has been operated with funding from the Japanese Ministry of Education, Science, Sports and Culture, and the U.S. Department of Energy.

* Deceased.

† also at BMCC/CUNY, Science Department, New York, New York, USA.

- [1] J. C. Pati and A. Salam, Phys. Rev. **D8**, 1240 (1973).
- [2] J. C. Pati and A. Salam, Phys. Rev. Lett. **31**, 661 (1973).
- [3] H. Georgi and S. Glashow, Phys.Rev.Lett. **32**, 438 (1974).
- [4] H. Fritzsch and P. Minkowski, Annals Phys. **93**, 193 (1975).
- [5] C. McGrew, R. Becker-Szendy, C. Bratton, J. Breault, D. Cady, et al. (IMB-3 Collaboration), Phys.Rev. **D59**, 052004 (1999).
- [6] K. Hirata et al. (KAMIOKANDE-II Collaboration), Phys.Lett. **B220**, 308 (1989).
- [7] M. Shiozawa et al. (Super-Kamiokande Collaboration), Phys.Rev.Lett. **81**, 3319 (1998), hep-ex/9806014.
- [8] K. Kobayashi et al. (Super-Kamiokande Collaboration), Phys.Rev. **D72**, 052007 (2005), hep-ex/0502026.
- [9] P. Nath and P. Fileviez Perez, Phys.Rept. **441**, 191 (2007), hep-ph/0601023.
- [10] G. Fogli, E. Lisi, A. Marrone, D. Montanino, and A. Palazzo, Phys.Rev. **D66**, 053010 (2002), hep-ph/0206162.
- [11] V. Takhistov et al. (Super-Kamiokande Collaboration), Phys.Rev.Lett. **113**, 101801 (2014), 1409.1947.
- [12] J. Learned, F. Reines, and A. Soni, Phys.Rev.Lett. **43**, 907 (1979).
- [13] M. Cherry, M. Deakyne, K. Lande, C. Lee, R. Steinberg, et al., Phys.Rev.Lett. **47**, 1507 (1981).
- [14] K. Olive et al. (Particle Data Group), Chin.Phys. **C38**, 090001 (2014).
- [15] D. Silverman and A. Soni, Phys.Lett. **B100**, 131 (1981).
- [16] J. M. Arnold, B. Fornal, and M. B. Wise, Phys.Rev. **D88**, 035009 (2013), 1304.6119.
- [17] L. Canetti, M. Drewes, and M. Shaposhnikov, New J.Phys. **14**, 095012 (2012), 1204.4186.
- [18] A. Sakharov, Pisma Zh.Eksp.Teor.Fiz. **5**, 32 (1967).
- [19] C. Berger et al. (Frejus Collaboration), Phys.Lett. **B269**, 227 (1991).
- [20] T. Araki et al. (KamLAND Collaboration), Phys.Rev.Lett. **96**, 101802 (2006), hep-ex/0512059.
- [21] M. Litos, K. Abe, Y. Hayato, T. Iida, M. Ikeda, et al., Phys.Rev.Lett. **112**, 131803 (2014).
- [22] R. N. Mohapatra and G. Senjanovic, Phys.Rev.Lett. **49**, 7 (1982).
- [23] L. Arnellos and W. J. Marciano, Phys.Rev.Lett. **48**, 1708 (1982).
- [24] D. Bryman, Phys.Lett. **B733**, 190 (2014), 1404.7776.
- [25] Y. Fukuda et al. (Super-Kamiokande Collaboration), Nucl.Instrum.Meth. **A501**, 418 (2003).
- [26] K. Abe et al., Nucl.Instrum.Meth. **A737**, 253 (2014), 1307.0162.
- [27] K. Abe et al. (Super-Kamiokande Collaboration) (2013), 1305.4391.
- [28] K. Choi et al. (Super-Kamiokande), Phys.Rev.Lett. **114**, 141301 (2015), 1503.04858.
- [29] T. Yamazaki and Y. Akaishi, Phys.Lett. **B453**, 1 (2000).
- [30] H. Nishino et al. (Super-Kamiokande), Phys.Rev. **D85**, 112001 (2012), 1203.4030.
- [31] C. Regis et al. (Super-Kamiokande Collaboration), Phys.Rev. **D86**, 012006 (2012), 1205.6538.
- [32] K. Abe et al. (Super-Kamiokande Collaboration), Phys.Rev. **D90**, 072005 (2014), 1408.1195.
- [33] J. Gustafson et al. (Super-Kamiokande), Phys.Rev. **D91**, 072009 (2015), 1504.01041.
- [34] K. Nakamura, S. Hiramatsu, T. Kamae, H. Muramatsu, N. Izutsu, et al., Nucl.Phys. **A268**, 381 (1976).
- [35] R. Brun, F. Carminati, and S. Giani (1994).
- [36] S. Jadach, Z. Was, R. Decker, and J. H. Kuhn, Comput.Phys.Commun. **76**, 361 (1993).
- [37] M.-C. Chen and V. Takhistov, Phys.Rev. **D89**, 095003 (2014), 1402.7360.
- [38] M. Honda, T. Kajita, K. Kasahara, S. Midorikawa, and T. Sanuki, Phys.Rev. **D75**, 043006 (2007), astro-ph/0611418.
- [39] Y. Hayato, Nucl.Phys.Proc.Suppl. **112**, 171 (2002).
- [40] K. Abe et al. (Super-Kamiokande), Phys. Rev. **D91**, 052019 (2015), 1410.2008.
- [41] M. Shiozawa (Super-Kamiokande Collaboration), Nucl.Instrum.Meth. **A433**, 240 (1999).
- [42] R. Wendell et al. (Super-Kamiokande Collaboration), Phys.Rev. **D81**, 092004 (2010), 1002.3471.